JCI insight

Regulation of bile duct epithelial injury by hepatic CD71^{+} erythroid cells

Li Yang, … , Zhenhua Luo, Jorge A. Bezerra

JCI Insight. 2020;5(11):e135751. https://doi.org/10.1172/jci.insight.135751.

Research Article Hepatology

Graphical abstract

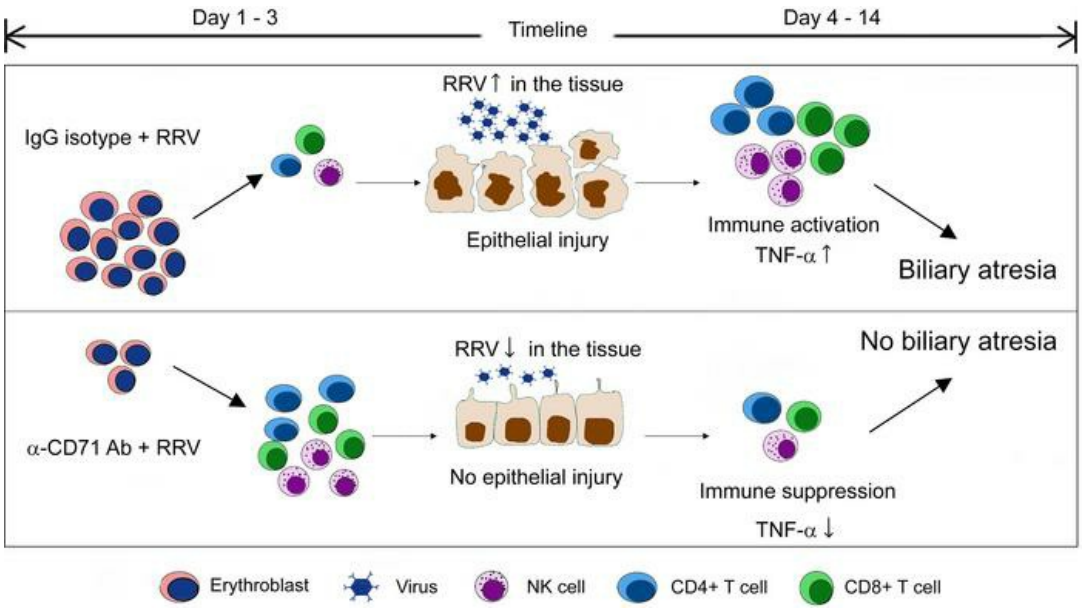

JCI insight

RESEARCH ARTICLE

Regulation of bile duct epithelial injury by hepatic CD71$^+$ erythroid cells

Li Yang,[1,2] Pranavkumar Shivakumar,[1] Jeremy Kinder,[3] Sing Sing Way,[3] Bryan Donnelly,[4] Reena Mourya,[1] Zhenhua Luo,[1,5] and Jorge A. Bezerra[1]

[1]Division of Gastroenterology, Hepatology and Nutrition, Cincinnati Children's Hospital Medical Center (CCHMC) and Department of Pediatrics, University of Cincinnati College of Medicine, Cincinnati, Ohio, USA. [2]Division of Pediatric Surgery, Union Hospital, Tongji Medical College, Huazhong University of Science and Technology, Wuhan, Hubei, China. [3]Division of Infectious Diseases and Perinatal Institute and [4]Division of Pediatric and Thoracic Surgery, CCHMC, Ohio, USA. [5]Institute of Precision Medicine, The First Affiliated Hospital, Sun Yat-sen University, Guangzhou City, Guangdong, China.

Extramedullary hematopoietic cells are present in the liver of normal neonates in the first few days of life and persist in infants with biliary atresia. Based on a previous report that liver genes are enriched by erythroid pathways, we examined the liver gene expression pattern at diagnosis and found the top 5 enriched pathways are related to erythrocyte pathobiology in children who survived with the native liver beyond 2 years of age. Using immunostaining, anti-CD71 antibodies identified CD71$^+$ erythroid cells among extramedullary hematopoietic cells in the livers at the time of diagnosis. In mechanistic experiments, the preemptive antibody depletion of hepatic CD71$^+$ erythroid cells in neonatal mice rendered them resistant to rhesus rotavirus–induced (RRV-induced) biliary atresia. The depletion of CD71$^+$ erythroid cells increased the number of effector lymphocytes and delayed the RRV infection of livers and extrahepatic bile ducts. In coculture experiments, CD71$^+$ erythroid cells suppressed the activation of hepatic mononuclear cells. These data uncover an immunoregulatory role for CD71$^+$ erythroid cells in the neonatal liver.

Introduction

Biliary atresia (BA) presents with a rapidly progressive inflammation, fibrosis, and obstruction of extrahepatic bile ducts (EHBDs) in early infancy (1). Studies in animal models and human tissues suggest the injury of intrahepatic and EHBDs is biologically linked to DCs, NK cells, and CD8$^+$ T cells, as well as myeloid cells that accumulated in neonatal liver (2–7). In neonatal mice, the injury of bile ducts occurs as early as day 1 after infection with rhesus rotavirus (RRV), preceding the onset of cholestasis and bile duct obstruction (8). With a low number of Tregs in the first 3 days of life, RRV promotes the activation of hepatic DCs, NK cells, and T lymphocytes (7) and requires $\alpha_2\beta_1$-integrin by cholangiocytes for the full expression of the BA phenotype in newborn mice (9). In addition to the population of the neonatal liver by immune cells, the presence of extramedullary hematopoietic cells is a common finding in liver biopsies at the time of diagnosis of BA (10, 11).

Although the precise phenotype of hepatic hematopoietic cells is not fully understood, some cells express CD71 (transferrin receptor, *TFRC* gene) and TER119 (erythroid lineage molecule, *GYPA* gene, CD235a in human). Here termed CD71$^+$ erythroid cells, these cells play an important role in the regulation of the developing neonatal immune system (12, 13), including the suppression of the neonatal response to pathogenic and commensal microorganisms during the transition to the extrauterine environment (14). CD71$^+$ erythroid cells use arginase-2 and direct cell contact to inhibit lymphocytes and myeloid cells, potentially skewing the expression of cytokines toward a Th2 commitment (15, 16). In mice, the depletion of these cells by the administration of anti-CD71 antibodies allows for the activation of neonatal myeloid and NK cells and clearance of *L. monocytogenes* and *E. coli* (17, 18). Based on these properties, we hypothesized that hepatic CD71$^+$ erythroid cells regulate the immune response that injures the duct epithelium. Using the model of RRV-induced experimental BA in mice, we found that depletion of CD71$^+$ erythroid cells protect mice from bile duct injury and obstruction by the attenuation of immune cells and the timely clearance of the virus from the liver and bile ducts.

Conflict of interest: The authors have declared that no conflict of interest exists.

Submitted: December 17, 2019
Accepted: April 29, 2020
Published: May 14, 2020.

Reference information: *JCI Insight*. 2020;5(11):e135751. https://doi.org/10.1172/jci.insight.135751.

Results

Gene signature is enriched for erythrocyte-associated pathways in children surviving with native livers. We reported recently that liver gene expression profiling at diagnosis identifies children with BA likely to be alive with the native liver at 2 years of age (19). Among the gene groups were those related to erythrocyte function. For an in-depth analysis of these genes or gene groups, we analyzed the mRNA expression data for the entire cohort of 171 BA patients by identifying genes that changed by 1.5-fold between the patients who survived with their native liver or those who died or required liver transplantation. A total of 26 genes were significantly upregulated in surviving patients, with functional enrichment analyses of the top 5 pathways relating to erythrocyte pathobiology ($-\log_{10}$(FDR) > 2; Figure 1). In contrast, the genes upregulated in the low-survival group did not show any enriched pathways (Supplemental Table 1; supplemental material available online with this article; https://doi.org/10.1172/jci.insight.135751DS1). These data suggest a biological link between the erythroid lineage population in the liver and pathogenesis of BA.

CD71$^+$ erythroid cells reside in human and mouse livers and increase after RRV infection. To explore the potential role of erythroid cells in disease pathogenesis, we first investigated whether the CD71$^+$ erythroid cells are present among extramedullary hematopoietic cells that populate the liver at the time of diagnosis of BA (Figure 2A). Using dual-staining immunofluorescence, the liver contained cells double-positive for CD71 and CD235a (Figure 2B). Using anti-CD71 antibodies, single-antibody IHC showed these cells to reside within foci of extramedullary hematopoiesis in human livers and in livers of neonatal mice with administration of saline or RRV at 1 day of age (Figure 2C).

To explore the potential role of CD71$^+$ erythroid cells in pathogenesis of BA, we first used FACS to quantify cells that were double-stained for CD71$^+$ and TER119$^+$ (the murine homolog of human 235a) in hepatic mononuclear cells harvested at 1, 3, and 7 days after RRV or saline injection. RRV induced a transient but statistically significant surge of hepatic CD71$^+$Ter119$^+$ cells within 1 day (RRV, 64% ± 2.7%; saline, 53% ± 5.7%; $P = 0.04$), with a return to the saline-control liver by 3 days (RRV, 40.0% ± 3.9%; saline, 40.7% ± 1.0%; $P = 0.87$) and below saline-control liver at 7 days (RRV, 5.7% ± 1.2%; saline, 13.9% ± 2.2%; $P = 0.0006$) (Figure 2, D and E). This increase was the first indication that CD71$^+$ erythroid cells may represent a biologically relevant response to RRV challenge.

Preemptive depletion of CD71$^+$ erythroid cells suppresses bile duct injury. To investigate if the increase in hepatic CD71$^+$ erythroid cells plays a mechanistic role in bile duct injury in experimental BA, we examined the clinical symptoms and bile duct injury induced by RRV infection in neonatal mice depleted of CD71$^+$ erythroid cells. First, to precisely define the level of depletion of CD71$^+$ erythroid cells, we administered 20 μg of anti-CD71 depleting antibody i.p. to newborn mice and quantified CD71$^+$ erythroid cells by FACS. This strategy decreased levels of CD71$^+$/Ter119$^+$ cells at 1 day (20.6% ± 1.4% versus 51.4% ± 2.4%, $P < 0.0001$) and 3 days (27.8% ± 4.1% versus 53.7% ± 3.3%, $P = 0.0028$) after injection when compared with mice administered rat IgG isotype as controls; anti-CD71 antibodies had a small effect on the number of these cells in the spleen (Figure 3, A and B).

Using the same protocol, we administered anti-CD71 antibody soon after birth, followed by RRV injection 24 hours later. Mice injected with anti-CD71 antibody had significantly better weight gain compared with isotype controls, had only 23.8% incidence of jaundice, and had improved survival to 57.1% at 3 weeks of life, compared with 18.7% survival of RRV-infected control mice that received rat IgG isotype control (Figure 3C). Investigating the liver to determine the basis for the improved clinical outcome, we found a decrease in inflammation and expansion of portal tracts in mice receiving anti-CD71 antibody at 7 and 11 days after RRV (Figure 3D). At the same time points, EHBDs showed less inflammation, largely intact epithelial layer, and patent lumen in 78.6% of the mice, which differed substantially from mice infected with RRV but not receiving anti-CD71 antibody (0% of them with patent lumen). These data show that preemptive depletion of CD71$^+$ erythroid cells significantly decreased bile duct inflammation, maintained patency of EHBDs, and improved survival in RRV-infected mice.

Increases in effector immune cells within 24 hours of infection. To understand the mechanisms of improved phenotype induced by the depletion of CD71$^+$ erythroid cells, we quantified the population of immune cells after RRV based on the previous reports that CD71$^+$ erythroid cells suppress neonatal T lymphocytes and NK cells (18, 20). Twenty-four hours after infection, anti-CD71 antibodies prevented the rise of CD71$^+$ TER119$^+$ cells (10.0% ± 3.4% versus 30.7% ± 2.8%, $P = 0.003$) after RRV (Figure 4A) and allowed for a surge in CD4$^+$ T cells (15.5% ± 0.8% versus 3.3% ± 0.6%, $P < 0.0001$), CD8$^+$ T cells (21.2% ± 0.6% versus 9.2% ± 2.2%, $P = 0.006$), and activated NK cells (56.2% ± 0.9% versus 41.8% ± 3.4%, $P = 0.0066$)

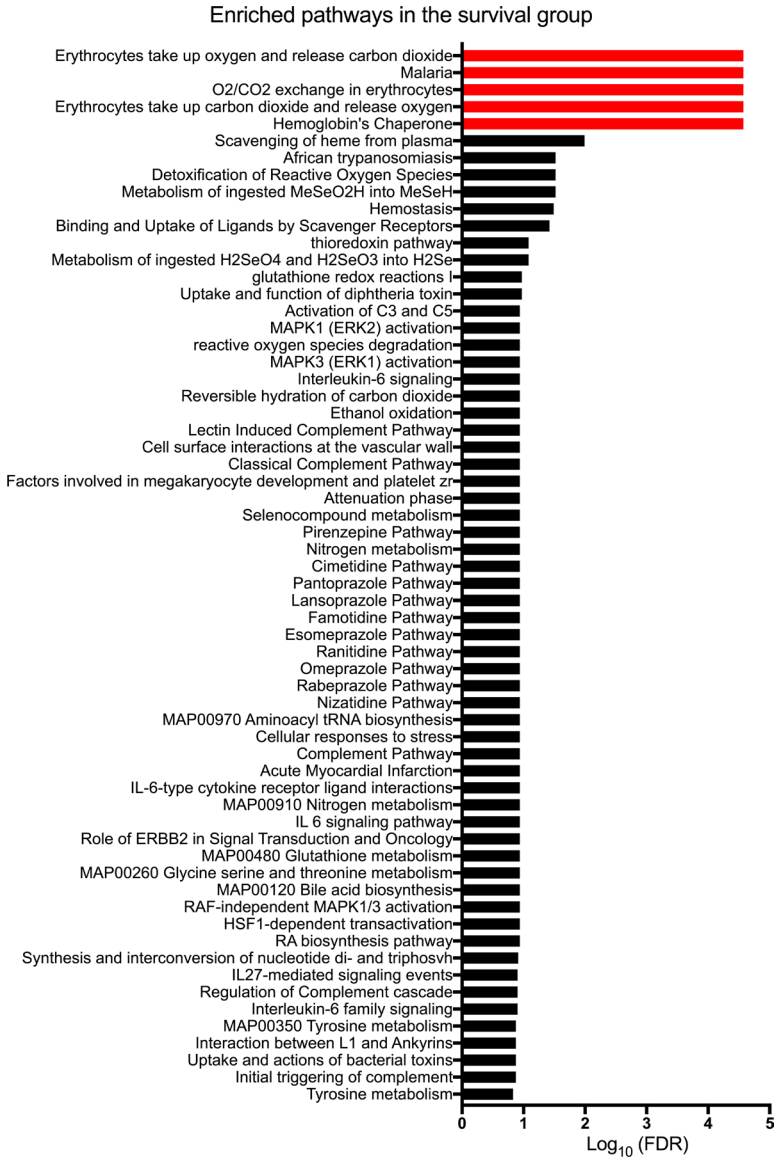

Figure 1. Enriched pathways of upregulated genes in patients surviving with native livers. Gene expression data for 171 patients with biliary atresia were divided into 2 groups: (a) survival with native liver at 2 years of age and (b) transplant or death before 2 years. Differentially expressed genes were identified by Cuffdiff 2, with the fold-change cutoff at 1.5 or higher and Benjamini-Hochberg FDR-adjusted $P < 0.05$. The list of genes upregulated in the survival group were further subjected to functional enrichment analysis shown above, with the top 5 significantly enriched pathways in red being related to erythrocyte pathobiology.

(Figure 4, B and C). These data support a potential role of CD71$^+$ erythroid cells in suppressing hepatic immune cells in the immediate neonatal period. The data also raise the possibility that an early inflammatory response may have suppressed the RRV infection of the hepatobiliary system.

Loss of CD71$^+$ erythroid cells delays the virus infection in the liver and EHBD. To examine the potential mechanisms of the improved phenotype induced by the depletion of CD71$^+$ erythroid cells, we determined whether anti-CD71 antibodies interfered with the ability of RRV to infect cholangiocytes. We found that preincubation of RRV or cholangiocytes with anti-CD71 antibodies or IgG controls had no effect on the ability of RRV to infect cholangiocytes (Figure 5, A and B). Next, to investigate whether the increases in hepatic mononuclear cells induced by the depletion of CD71$^+$ erythroid cells suppressed RRV infection of the hepatobiliary system, we quantified RRV in liver and EHBD at days 3 and 7 after RRV infection in mice injected with anti-CD71$^+$ erythroid cells or IgG controls. RRV titers at 3 days after infection were lower in the liver and EHBD of mice receiving anti-CD71 antibodies and increased at day 7 in both tissues

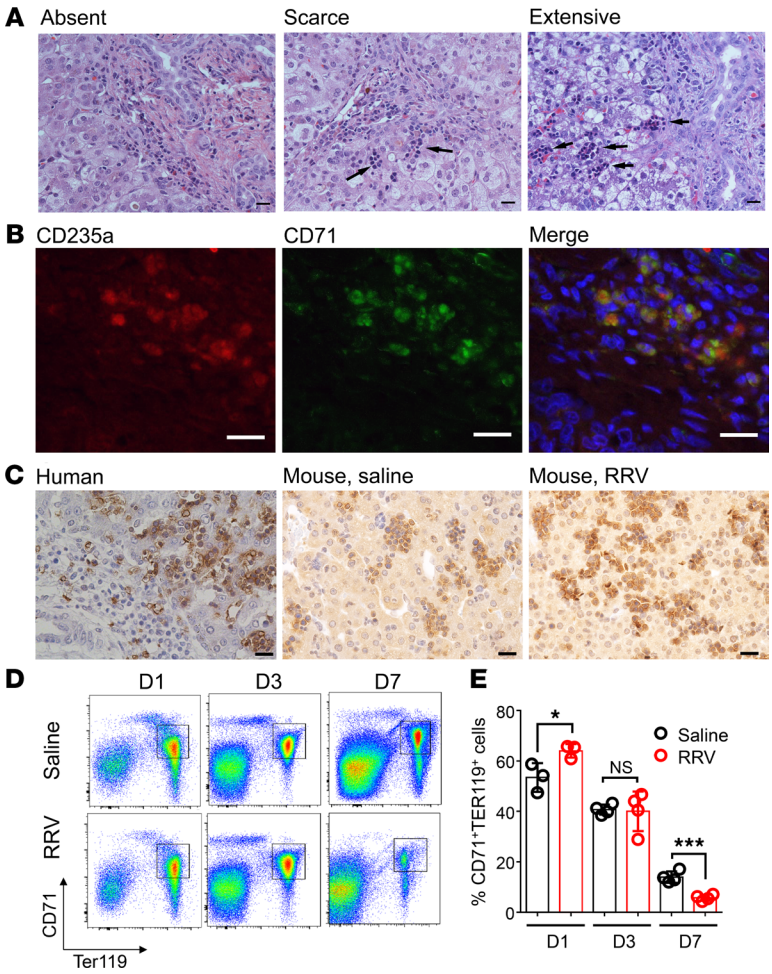

Figure 2. Localization of erythroblasts in liver tissues. (**A**) H&E staining of liver biopsies at the time of diagnosis of biliary atresia shows variable population of extramedullary cells (absent, scarce, or extensive cell clusters). Scale bar: 20 μM. (**B**) Immunofluorescence staining of surface markers, CD235a and CD71, identifies erythroblasts among hematopoietic cells. Scale bar: 20 μM. (**C**) Immunohistochemical staining using anti-CD71 antibody shows similar features in livers of a human neonate and newborn mice. The human liver tissue was obtained at the time of autopsy of a neonate without liver disease, and the mouse livers were obtained from saline- or RRV-injected neonatal mice at 1 day old. Scale bar: 20 μM. (**D** and **E**) Quantification of hepatic erythroblasts in response to RRV infection by using flow cytometry after incubation with anti-CD71 and anti-TER119 antibodies at days 1, 3, and 7 after injection of RRV or saline. $^{*}P < 0.05$, $^{***}P < 0.001$. Differences in mean values were statistically analyzed by 2-tailed Student's *t* test. $n = 3$–4/group.

compared with isotype controls (Figure 5, C and D). This lower RRV titer in EHBDs and livers early after infection raised the possibility that the virus suppression may be due to an increase in inflammatory cells that were no longer under the immunosuppression of CD71$^+$ erythroid cells.

Because Tregs provide important immune suppressive functions, we compared the relative abundance of Tregs and CD71$^+$ erythroid cells at day 3 and day 7 after RRV infection. Immunostaining with anti-CD71 and anti-Foxp3 antibodies showed an absence of hepatic Tregs and abundant CD71$^+$ erythroid 3 days after RRV infection, with both cell types being present at low numbers at 7 days (Supplemental Figure 1). These data indicate hepatic CD71$^+$ erythroid cells might play an important role in immune suppression in the immediate postnatal period when Tregs are still largely absent.

Neonatal CD71$^+$ erythroid cells suppress mononuclear cells. To directly test if hepatic CD71$^+$ erythroid cells suppress the activation of inflammatory cells, we cocultured neonatal CD71$^+$ erythroid cells from the neonatal liver (as effector cells) with hepatic mononuclear cells from 8-week-old mice (as responder cells) at a 1:1 ratio, and the concentration of TNF-α in supernatant was measured after 72 hours of stimulation with anti–mouse CD3 antibody. Responder cells increased the expression of TNF-α upon stimulation, but when cocultured with neonatal CD71$^+$ erythroid cells, TNF-α production was

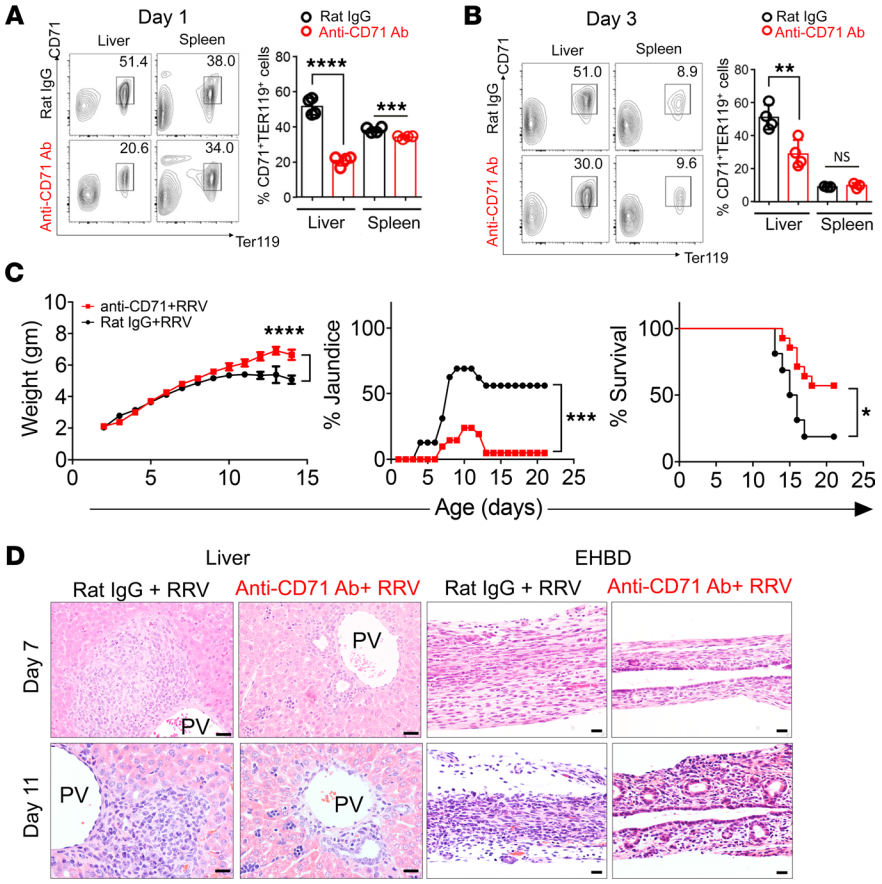

Figure 3. Phenotypic changes induced by the depletion of CD71⁺ cells in RRV-infected mice. (**A** and **B**) Flow cytometry plots and graphical quantification of CD71⁺Ter119⁺ erythroblasts after anti-CD71 antibody or rat IgG injection within 12 hours of birth. Livers or extrahepatic bile ducts (EHBD) were harvested at day 1 and day 3 after injection. $^{**}P < 0.01$, $^{***}P < 0.001$, $^{****}P < 0.0001$, $n = 4$ for each group. (**C**) Weight, jaundice, and survival percentage after the administration of anti-CD71 antibody or isotype (rat IgG) into newborn mice, followed by the i.p. administration of RRV 24 hours later. Two-tailed Student's *t* test was used for weight comparison, and χ^2 test was used for jaundice percentage. $^{*}P < 0.05$, $^{***}P < 0.001$, $^{****}P < 0.0001$; Kaplan-Meier survival curve was analyzed by the log-rank (Mantel-Cox) test; $n = 16$ for Rat IgG group and $n = 21$ for anti-CD71 antibody group. (**D**) H&E staining of liver and EHBD at days 7 and 11 after RRV infection. $n = 5$ for rat IgG–treated group and $n = 14$ for anti-CD71 antibody–treated group. PV, portal vein. Scale bar: 20 μM.

significantly reduced (Figure 6). These data suggest that neonatal CD71⁺ erythroid cells suppress the activation of hepatic mononuclear cells.

Repopulation by CD71⁺ erythroid cells promotes long-term survival. Last, we reasoned that if CD71⁺ erythroid cells have immunosuppressive properties, they would need to repopulate the neonatal liver after antibody injection in order to suppress the activation of effector lymphocytes. To investigate this possibility, we designed an experiment to reproduce the RRV model with and without pretreatment with depleting anti-CD71 antibodies, along with a third group that received a second dose of anti-CD71 antibodies the day after RRV inoculation (Figure 7A). Quantification of CD71⁺ erythroid cells 3 days after RRV inoculation showed a rebound after a single dose of anti-CD71 antibodies that was significantly higher than the increase induced by the RRV infection. Notably, the second dose of anti-CD71 antibodies promoted a significant cell depletion, jaundice in > 90% of mice, and early mortality (Figure 7, B and C). Quantifying the population of hepatic mononuclear cells between the groups of 1 and 2 antibody injections, we found a significant increase in CD4⁺ and CD8⁺ T cells and NK lymphocytes in mice with the second antibody injection (Figure 7D). These data support the role of CD71⁺ cells in suppression of hepatic effector cells to prevent further liver injury.

Discussion

We found that CD71⁺ erythroid cells populate the neonatal liver at birth and further increase in response to RRV infection. The depletion of these cells by the administration of anti-CD71 antibodies within 24 hours

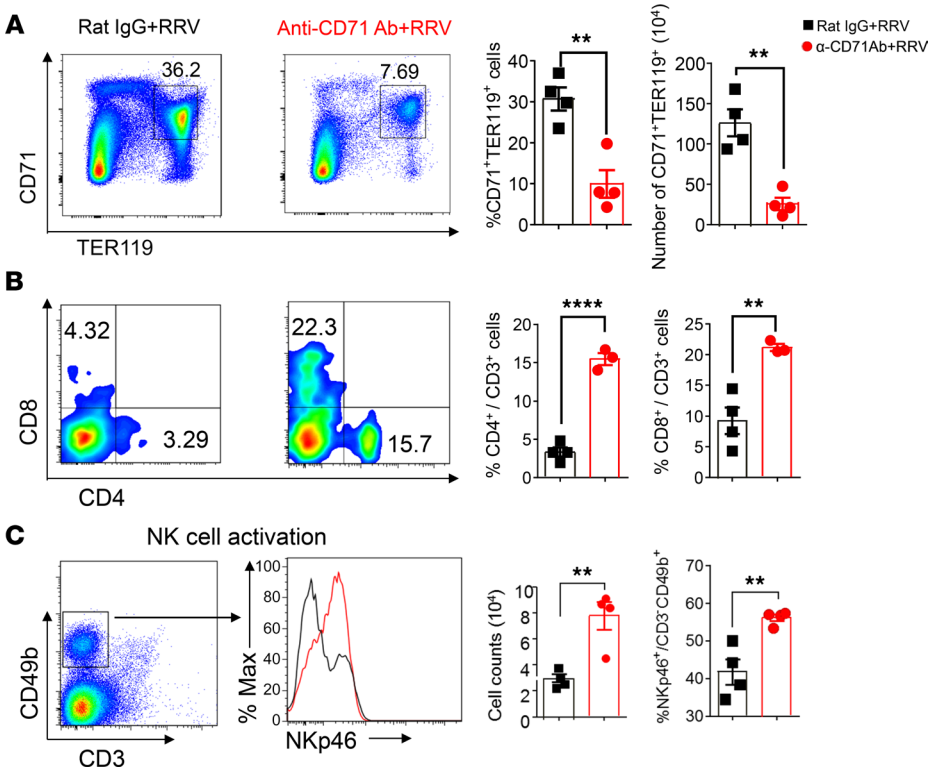

Figure 4. Increases of effector immune cells 24 hours after depletion of CD71⁺ erythroid cells. (**A–C**) Representative plots and quantification of CD71⁺Ter119⁺ cells (**A**), CD4⁺ T cells and CD8⁺ T cells (**B**), and activation marker NKp46 in CD3⁻CD49b⁺ cells and total NK cell counts (**C**) in livers of RRV-infected mice pretreated with either rat IgG or anti-CD71 antibody. Differences in mean values analyzed by 2-tailed Student's *t* test; $^{**}P < 0.01$; $^{****}P < 0.0001$; $n = 4$/group.

of birth triggered an immediate increase in effector immune cells in the liver, decreased the tissue viral load, and minimized cholangiocyte injury of EHBDs. This initial response was accompanied by a subsequent decrease in the number of hepatic inflammatory cells, maintained patency of bile ducts, and improved long-term survival of neonatal mice. Quantifying the temporal dynamics of hepatic CD71⁺ erythroid cells after RRV infection, we found that the number of these cells increased and restored previous numbers within 3 days. Blocking this surge by a new administration of anti-CD71 antibodies allowed hepatic inflammatory cells to injure the bile duct epithelium and obstruct the bile ducts, manifesting the high mortality that is typical of experimental BA. These data are in keeping with an immunosuppressive role of hepatic CD71⁺ erythroid cells in the regulation of the immediate response of the neonatal immune system to a virus insult and the ability to suppress an inflammatory injury of bile ducts in early postnatal life.

The response of the neonatal immune system to RRV infection is a central pathogenic mechanism of BA. Upon virus exposure, cells of the innate and adaptive immune systems increase in the liver and EHBDs (21–25). In fact, an early increase of neutrophils and plasmacytoid DCs upon RRV infection and their release of IL-8 and IL-15 indirectly drive epithelial injury by activating NK lymphocytes, as reported previously in studies using protein depletion and gene activation in mice (2, 26, 27). In adoptive transfer experiments, Tregs were shown to suppress this immune response and to largely prevent the BA phenotype (6, 7). These experiments also showed that the absence of Tregs in the first 3 days of life makes neonatal mice susceptible to an uncontrolled activation of immune cells, which, in the BA model, is responsible for tissue injury (7). In this context, the ability of resident CD71⁺ erythroid cells to block the activation of mononuclear cells raises the possibility that they may fill the immunoregulatory deficit created by the transient lack of Tregs in the immediate postnatal period. Despite a recent study reporting an interplay between CD71⁺ erythroid cells and Tregs (28), we found that the highest population of hepatic CD71⁺ cells 3 days after RRV infection was not accompanied by a discernable number of Tregs. The existence of a crosstalk between these 2 cells and the potential for functional synergy require more in-depth analysis in future studies.

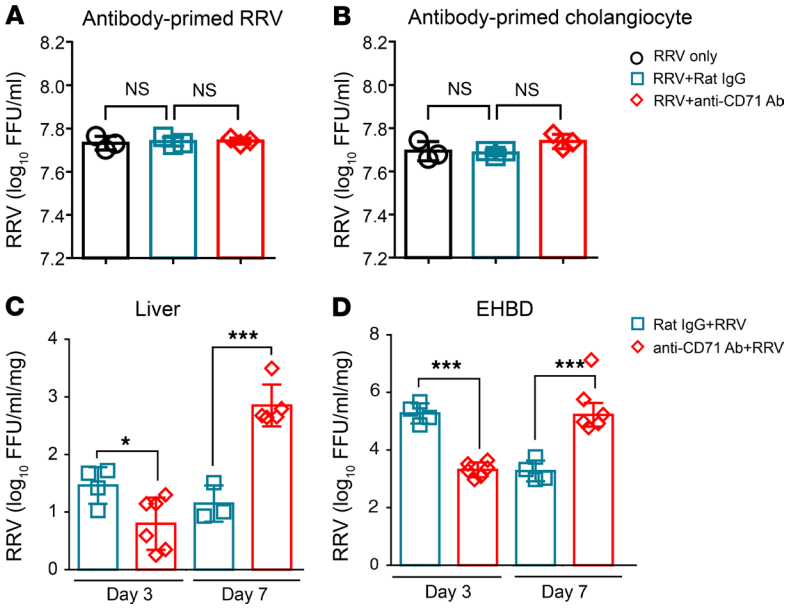

Figure 5. RRV quantification in vitro and in mouse tissues in the presence of anti-CD71 antibodies. (**A** and **B**) RRV (**A**) or cholangiocytes (**B**) were preincubated with anti-CD71 antibody or rat IgG isotypes for 1 hour and then subjected to a RRV-cholangiocyte culture system for 24 hours, at which time RRV titer was quantified. Significance was assessed by 1-way ANOVA; n = 3–4/group. (**C** and **D**) RRV titer was measured from homogenized livers (**C**) and extrahepatic bile ducts (EHBD) (**D**) harvested at days 3 and 7 after RRV injection into neonatal mice. Data were analyzed by 2-tailed Student's t test; $^*P < 0.05$; $^{***}P < 0.001$; n = 3–6/group.

In nonhepatic tissues, CD71$^+$ erythroid cells modulate the immune response to bacterial infection, gut microbiome colonization, fetal-maternal tolerance, and carcinogenesis (15, 17, 18, 29, 30). Our data expand their suppressive roles to immune cells of the neonatal liver, with a direct link to mechanisms driving the hepatobiliary injury induced by an exposure to rotavirus soon after birth. The population of human and murine livers by hematopoietic cells at birth has been interpreted as residual extramedullary hematopoiesis that spontaneously ends in the first week of life. Here, we show that these cells are biologically relevant and contain CD71$^+$ cells, whose depletion allows hepatic mononuclear cells to undergo activation upon virus exposure. Soon after cellular activation, CD71$^+$ cells repopulate the liver within 3 days and suppress immune cells; if such a repopulation is blocked by the administration of a new dose of anti-CD71 antibodies, hepatic inflammatory cells injure the bile duct epithelium, promote lumen obstruction, and allow for the full expression of the BA phenotype. The demonstration of these biological events in our studies support a biological role of CD71$^+$ erythroid cells in the regulation of the immune response of the neonatal liver to exogenous insults. CD71$^+$ erythroid cells in humans are reported to be a major source of ROS, and the role of ROS in BA was reported previously (31–34). This implies CD71$^+$ erythroid cells can play a role in BA not only through immune suppression, but also through other mechanisms, such as the regulation of ROS production, which require further investigation.

In summary, we report that extramedullary hematopoiesis of neonatal livers contains CD71$^+$ erythroid cells with unique immunosuppressive properties to hepatic mononuclear cells. We provide

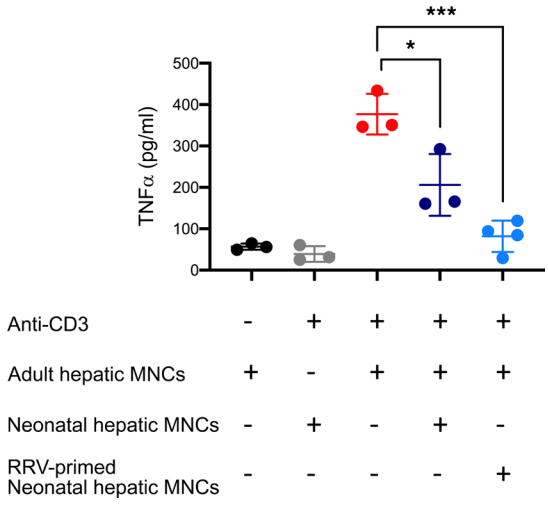

Figure 6. Suppression of adult hepatic mononuclear cells by neonatal hepatic mononuclear cells. Adult hepatic mononuclear cells (MNCs) can produce TNF-α upon anti-CD3 stimulation; therefore, they were used as responder cells. Neonatal liver harvested at 24 hours of life, or 3 days after antibody depletion followed by RRV infection, was used as erythroblast pool to function as effector cells. TNF-α levels were measured in supernatant 72 hours after coculture. "+" denotes presence. "–" denotes absence. One-way ANOVA test was performed. $^*P < 0.05$, $^{***}P < 0.001$. n = 3/group.

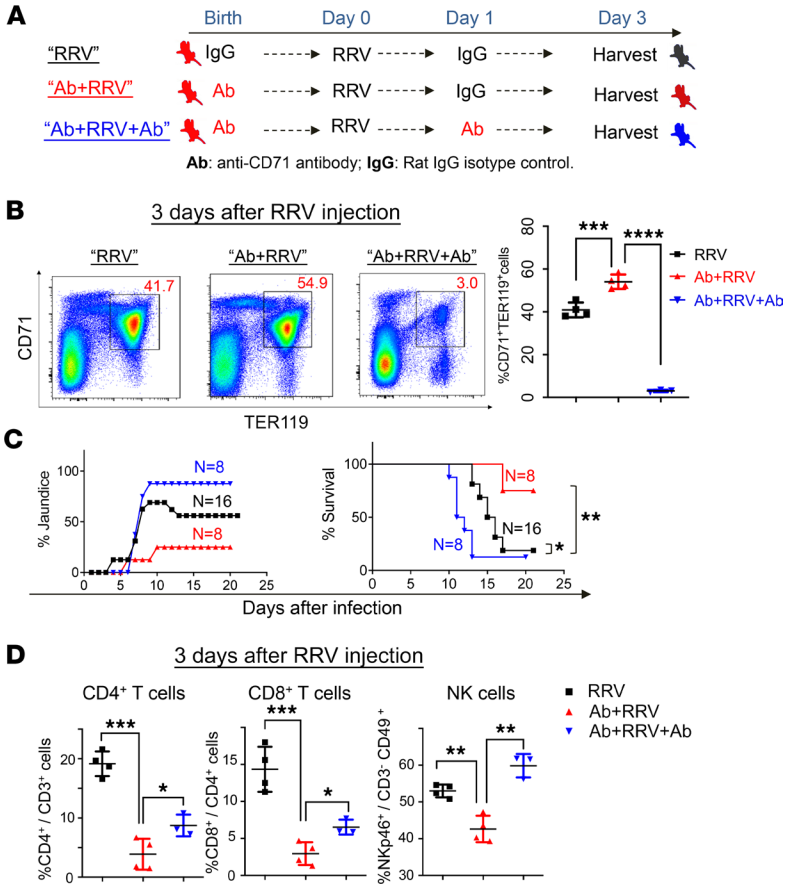

Figure 7. Continuous depletion of CD71⁺ cells worsens the biliary atresia phenotype. (**A**) Schematic diagram of the injection timeline for anti-CD71 antibodies or rat IgG isotypes into newborn mice. (**B**) The quantification of hepatic CD71⁺Ter119⁺ cells by flow cytometry shows the prevention of the 3-day surge after RRV infection. Data were analyzed by 1-way ANOVA; ***P < 0.001; ****P < 0.0001; n = 4/group. (**C**) Jaundice and survival differences in 3 groups. Kaplan-Meier survival curve were analyzed by log-rank (Mantel-Cox) test; *P < 0.05; **P < 0.01; n = 8-16 in each group. (**D**) CD4⁺ T cells, CD8⁺ T cells, and NK cells were quantified by flow cytometry. Data were analyzed by 1-way ANOVA; *P < 0.05; **P < 0.01; ***P < 0.001; n = 3–4/group.

evidence that their ability to suppress hepatic immune cells renders neonatal mice susceptible to virus infection and the BA phenotype. This is supported by the low virus titer in the liver when mice are depleted of CD71⁺ erythroid cells. The immunoregulatory function of CD71⁺ erythroid cells is also is also evidenced by the ability to repopulate the liver, suppress immune cells, and protect the tissue from injury. We propose a unifying functional model in which CD71⁺ erythroid cells provide a immunosuppressive role during the immediate postnatal period, a time when the absence of Tregs makes neonatal mice unable to regulate the eventual activation of inflammatory cells as the organism enters the microbiota-rich extrauterine environment after birth. In humans, this is supported by an enrichment of gene groups related to erythroid function in children with BA surviving beyond 2 years of age. Altogether, these studies raise the possibility that the manipulation of CD71⁺ erythroid cells may represent a therapeutic target to block progression of liver disease in BA.

Methods

Human tissue and gene expression enrichment pathway analysis. Tissue sections were obtained from deidentified paraffin-embedded liver tissues obtained from children at the time of diagnosis of BA and archived in the biobank repository of CCHMC. RNA sequencing (RNAseq) data of 171 BA patients was retrieved from previous deposition in the Gene Expression Omnibus database under accession number GSE122340 (https://www.ncbi.nlm.nih.gov/geo/query/acc.cgi?acc=GSE122340) (19). For this analysis, we divided patients into 2 groups: survival with native liver at 2 years of age and transplant or death before 2 years. Differentially expressed genes were identified by Cuffdiff 2. Upregulated genes are defined as genes showing at least 1.5-fold upregulation, with P < 0.05.

A group of 13 upregulated genes was identified (Supplemental Table 1) and subjected to pathway analysis with ToppFun (https://toppgene.cchmc.org/enrichment.jsp). The significance of individual pathways in functional enriched analysis is defined as Benjamini and Hochberg–corrected $P < 0.01$ (or $-\log_{10}$ [FDR] > 2).

Experimental model of BA. Eight- to 12-week-old BALB/c mice were purchased as mating pairs from Charles River Laboratories. The disease model was created in newborn mice; thus, the sex was not identifiable. Neonatal mice were injected i.p. with 1.5×10^6 fluorescence focus units (ffu) of RRV in 20 μL of DMEM or an equal volume of normal saline (NS; serving as controls) within 24 hours of birth to induce experimental BA, as described previously (35).

Antibodies for depletion and flow cytometric analysis. For in vivo depletion of $CD71^+$ erythroid cells, 20 μg purified anti-CD71 antibody was administered i.p. within 24 hours of birth, similarly to what was described previously (17). The same amount of rat IgG2a isotype was administered to different mice to serve as controls. Mononuclear cells were isolated from livers of neonatal mice (35) and subjected to antibody staining for flow cytometric analysis, which was performed using FACS Canto II dual-laser flow cytometer (BD Biosciences), and the data were analyzed using FlowJo software (Tree Star Inc.). Fluorochrome-conjugated mouse antibodies were as follows: FITC-conjugated CD71 from eBioscience; APC-conjugated Cd8a and Pan-NK (CD49b) from Miltenyi Biotec; PerCP-conjugated CD3, CD4, CD49b, and anti-NKp46 antibody and BV605-conjugated CD3 and CD45 from BioLegend; and PE-conjugated TER119 from R&D Systems.(catalog FAB1125P).

Histopathology, IHC, and immunofluorescence. Livers and EHBD/gallbladder were harvested from neonatal mice using a dissecting microscope. Paraffin-embedded sections were examined after staining with H&E. To localize $CD71^+$ erythroid cells and Tregs in liver tissues from patients and experimental mice, IHC staining against CD71 (Invitrogen, catalog 13-6800) or against Foxp3 (Invitrogen, catalog 14-5773-80) was performed at a dilution of 1:100 in 4°C over night. For human samples, biotinylated anti-mouse antibody (Vector Laboratories) (catalog BP-9200) was used as a secondary antibody, followed by detection using avidin/biotin (VECTASTAIN ABC reagent PK-4001; Vector Laboratories) and the DAB substrate (Vector kit, SK-4100; Vector Laboratories). For mouse samples, the same anti-CD71 (Invitrogen, catalog 13-6800) was used in a mouse anti-mouse fashion with a Vector M.O.M. Kit (catalog BMK-2202). For CD235a (TER119) staining; mouse anti–human CD235a (Thermo Fisher Scientific, catalog MS-1843-R7) antibody was ready to use without dilution. Rat anti–mouse TER119 (Stemcell Technologies, catalog 60033) antibody were used at 1:200 dilutions for 1 hour at room temperature. For immunofluorescence staining, Dylight-488– (catalog 112-486-143) and -594–conjugated (catalog 112-517-003) secondary antibodies were obtained from Jackson ImmunoResearch.

RRV titer. RRV titers in EHBD/gallbladder and liver were determined in 96-well plates seeded with monkey kidney cells (cell line MA-104, information in Supplemental Table 1) using an antirotavirus hyper immune serum–based assay to quantify RRV ffu, as described previously (36).

Coculture and stimulation. Hepatic mononuclear cells from 1-day-old mice or 3 days after antibody depletion, followed by RRV infection, were used in coculture assays of immune activation as suppressor cells. Hepatic mononuclear cells from 8-week-old mice were used as responder cells. In these assays, 4×10^5 of responder cells were seeded into 96-well round-bottom plates individually or together with suppressor cells (neonatal hepatic mononuclear cells) at a 1:1 ratio and then stimulated for 72 hours with 0.125 μg/mL anti–mouse CD3 antibody (clone 145-2C11, BioXcell). The concentrations of TNF-α was measured by enzyme-linked immunosorbent assay (ELISA, R&D Systems).

Statistics. Statistical analysis of experimental data were performed using the GraphPad PRISM Version 8.3.0 (GraphPad Software). Values are expressed as mean ± SD. Differences in mean values of 2 groups were analyzed by 2-tailed Student's *t* test. Chi-square test was used to assess differences in the percentage of mice that developed jaundice between groups. Differences among 3 or more groups were analyzed by 1-way ANOVA. Kaplan-Meier survival curves were analyzed by log-rank test. Data are presented as mean ± SD. (*$P < 0.05$; **$P < 0.01$; ***$P < 0.001$; **** $P < 0.0001$).

Study approval. Animal studies were reviewed and approved by Cincinnati Children's IACUC (protocol no. IACUC2017-0007). Human samples were obtained after informed consent from patients' parents/legal guardians according to study protocols approved by Cincinnati Children's IRB.

Author contributions

Concept and design were contributed by LY, JAB, PS, JK, and SSW. Experiments and procedures were contributed by LY, BD, and RM. Writing of the manuscript was contributed by LY and JB. Data analysis was contributed by LY, ZL, and JAB.

Acknowledgments

This work is supported by NIH grants DK-64008 and DK-83781 to JAB and by the Gene Analysis Cores of the Digestive Health Center (DK-78392). We would like to acknowledge the assistance of the Research Flow Cytometry Core at Cincinnati Children's Hospital Medical Center.

Address correspondence to: Jorge A. Bezerra, Division of Gastroenterology, Hepatology and Nutrition, Cincinnati Children's Hospital Medical Center, 3333 Burnet Avenue, Cincinnati, Ohio 45229-3030, USA. Phone: 513.636.3008; Email: jorge.bezerra@cchmc.org.

1. Verkade HJ, et al. Biliary atresia and other cholestatic childhood diseases: Advances and future challenges. *J Hepatol*. 2016;65(3):631–642.
2. Saxena V, Shivakumar P, Sabla G, Mourya R, Chougnet C, Bezerra JA. Dendritic cells regulate natural killer cell activation and epithelial injury in experimental biliary atresia. *Sci Transl Med*. 2011;3(102):102ra94.
3. Liu YJ, et al. Dendritic Cells Regulate Treg-Th17 Axis in Obstructive Phase of Bile Duct Injury in Murine Biliary Atresia. *PLoS ONE*. 2015;10(9):e0136214.
4. Shivakumar P, et al. Effector role of neonatal hepatic CD8+ lymphocytes in epithelial injury and autoimmunity in experimental biliary atresia. *Gastroenterology*. 2007;133(1):268–277.
5. Okamura A, Harada K, Nio M, Nakanuma Y. Participation of natural killer cells in the pathogenesis of bile duct lesions in biliary atresia. *J Clin Pathol*. 2013;66(2):99–108.
6. Lages CS, Simmons J, Chougnet CA, Miethke AG. Regulatory T cells control the CD8 adaptive immune response at the time of ductal obstruction in experimental biliary atresia. *Hepatology*. 2012;56(1):219–227.
7. Miethke AG, Saxena V, Shivakumar P, Sabla GE, Simmons J, Chougnet CA. Post-natal paucity of regulatory T cells and control of NK cell activation in experimental biliary atresia. *J Hepatol*. 2010;52(5):718–726.
8. Oetzmann von Sochaczewski C, et al. Experimentally Induced Biliary Atresia by Means of Rotavirus-Infection Is Directly Linked to Severe Damage of the Microvasculature in the Extrahepatic Bile Duct. *Anat Rec (Hoboken)*. 2019;302(5):818–824.
9. Jafri M, et al. Cholangiocyte expression of alpha2beta1-integrin confers susceptibility to rotavirus-induced experimental biliary atresia. *Am J Physiol Gastrointest Liver Physiol*. 2008;295(1):G16–G26.
10. Russo P, et al. Key Histopathologic Features of Liver Biopsies That Distinguish Biliary Atresia From Other Causes of Infantile Cholestasis and Their Correlation With Outcome: A Multicenter Study. *Am J Surg Pathol*. 2016;40(12):1601–1615.
11. Moyer K, et al. Staging of biliary atresia at diagnosis by molecular profiling of the liver. *Genome Med*. 2010;2(5):33.
12. Cui L, Takada H, Takimoto T, Fujiyoshi J, Ishimura M, Hara T. Immunoregulatory function of neonatal nucleated red blood cells in humans. *Immunobiology*. 2016;221(8):853–861.
13. Elahi S. New insight into an old concept: role of immature erythroid cells in immune pathogenesis of neonatal infection. *Front Immunol*. 2014;5:376.
14. Dunsmore G, et al. Lower Abundance and Impaired Function of CD71+ Erythroid Cells in Inflammatory Bowel Disease Patients During Pregnancy. *J Crohns Colitis*. 2019;13(2):230–244.
15. Delyea C, et al. CD71$^+$ Erythroid Suppressor Cells Promote Fetomaternal Tolerance through Arginase-2 and PDL-1. *J Immunol*. 2018;200(12):4044–4058.
16. Rincon MR, Oppenheimer K, Bonney EA. Selective accumulation of Th2-skewing immature erythroid cells in developing neonatal mouse spleen. *Int J Biol Sci*. 2012;8(5):719–730.
17. Elahi S, et al. Immunosuppressive CD71+ erythroid cells compromise neonatal host defence against infection. *Nature*. 2013;504(7478):158–162.
18. Dunsmore G, Bozorgmehr N, Delyea C, Koleva P, Namdar A, Elahi S. Erythroid Suppressor Cells Compromise Neonatal Immune Response against *Bordetella pertussis*. *J Immunol*. 2017;199(6):2081–2095.
19. Luo Z, Shivakumar P, Mourya R, Gutta S, Bezerra JA. Gene Expression Signatures Associated With Survival Times of Pediatric Patients With Biliary Atresia Identify Potential Therapeutic Agents. *Gastroenterology*. 2019;157(4):1138–1152.e14.
20. Elahi S. Neglected Cells: Immunomodulatory Roles of CD71$^+$ Erythroid Cells. *Trends Immunol*. 2019;40(3):181–185.
21. Mack CL, Feldman AG, Sokol RJ. Clues to the etiology of bile duct injury in biliary atresia. *Semin Liver Dis*. 2012;32(4):307–316.
22. Glaser SS. Biliary atresia: is lack of innate immune response tolerance key to pathogenesis? *Liver Int*. 2008;28(5):587–588.
23. Mack CL. What Causes Biliary Atresia? Unique Aspects of the Neonatal Immune System Provide Clues to Disease Pathogenesis. *Cell Mol Gastroenterol Hepatol*. 2015;1(3):267–274.
24. Zagory JA, Nguyen MV, Wang KS. Recent advances in the pathogenesis and management of biliary atresia. *Curr Opin Pediatr*. 2015;27(3):389–394.
25. Averbukh LD, Wu GY. Evidence for Viral Induction of Biliary Atresia: A Review. *J Clin Transl Hepatol*. 2018;6(4):410–419.
26. Bessho K, et al. Gene expression signature for biliary atresia and a role for interleukin-8 in pathogenesis of experimental disease. *Hepatology*. 2014;60(1):211–223.
27. Shivakumar P, Sabla GE, Whitington P, Chougnet CA, Bezerra JA. Neonatal NK cells target the mouse duct epithelium via Nkg2d and drive tissue-specific injury in experimental biliary atresia. *J Clin Invest*. 2009;119(8):2281–2290.
28. Shahbaz S, et al. CD71+VISTA+ erythroid cells promote the development and function of regulatory T cells through TGF-β. *PLoS Biol*. 2018;16(12):e2006649.
29. Han Y, et al. Tumor-Induced Generation of Splenic Erythroblast-like Ter-Cells Promotes Tumor Progression. *Cell*. 2018;173(3):634–648.e12.
30. Zhao L, et al. Late-stage tumors induce anemia and immunosuppressive extramedullary erythroid progenitor cells. *Nat Med*. 2018;24(10):1536–1544.

31. Tiao MM, et al. Associations of mitochondrial haplogroups b4 and e with biliary atresia and differential susceptibility to hydrophobic bile Acid. *PLoS Genet*. 2013;9(8):e1003696.
32. Chen CJ, et al. The Characteristics of Antioxidant Activity after Liver Transplantation in Biliary Atresia Patients. *Biomed Res Int*. 2015;2015:421413.
33. Koh H, et al. Mitochondrial Mutations in Cholestatic Liver Disease with Biliary Atresia. *Sci Rep*. 2018;8(1):905.
34. Namdar A, et al. $CD71^+$ Erythroid Cells Exacerbate HIV-1 Susceptibility, Mediate *trans*-Infection, and Harbor Infective Viral Particles. *mBio*. 2019;10(6):e02767-19.
35. Yang L, et al. Regulation of epithelial injury and bile duct obstruction by NLRP3, IL-1R1 in experimental biliary atresia. *J Hepatol*. 2018;69(5):1136–1144.
36. Coots A, Donnelly B, Mohanty SK, McNeal M, Sestak K, Tiao G. Rotavirus infection of human cholangiocytes parallels the murine model of biliary atresia. *J Surg Res*. 2012;177(2):275–281.